Pressure Dependence of T_c to 17 GPa with and without Relaxation Effects in Superconducting $YBa_2Cu_3O_x$

S. Sadewasser and J. S. Schilling
Department of Physics, Washington University
C. B. 1105, One Brookings Dr., St. Louis, MO 63130

A. P. Paulikas and B. W. Veal
Materials Science Division, Argonne National Laboratory
9700 S. Cass Avenue, Argonne, IL 60439

July 28, 1999

Abstract

Hydrostatic high-pressure studies to 17 GPa were carried out on superconducting $YBa_2Cu_3O_x$ over the full range of oxygen content x. The observed bell-shaped $T_c(P)$-dependences are found to depend markedly on the temperature at which the pressure is changed. The time-dependent relaxation processes are studied using both T_c and the electrical resistivity at 298 K as probes. The activation volume for oxygen diffusion is determined from the pressure-dependent activation energy and compared with estimates from a simple hard-sphere model.

1 Introduction

For a given superconductor the dependence of T_c on pressure is of considerable interest since it contains information about the mechanism(s) responsible for the superconducting state itself. As does the isotope effect, the universal decrease of T_c with pressure in simple-metal superconductors (Sn, Al, In, etc.) points to the importance of electron-phonon coupling [1]. In transition metal superconductors the interpretation of the $T_c(P)$ data is more difficult since changes in both the lattice vibrational and electronic properties make significant contributions. In high-T_c superconductors (HTSC) the situation is considerably more complex since T_c depends sensitively on properties such as the carrier concentration, the degree of buckling in the CuO_2 plane(s), the occurrence of structural phase transitions, and pressure-induced relaxation phenomena.

In $YBa_2Cu_3O_y$ (Y-123) [2, 3], $Tl_2Ba_2CuO_{6+x}$ (Tl-2201) [4, 5, 6], and other high-T_c superconductors [7] the initial dependence of T_c on pressure often depends markedly on the pressure-temperature history of the sample. The relaxation phenomena responsible for this behavior are believed to originate from pressure-induced ordering of mobile oxygen defects in the lattice; the value of T_c appears to be a sensitive function of both the *concentration* and the *arrangement* of these defects. It is important to gain an understanding of these complex structural phenomena before comparing experimental data with the predictions of theoretical models which generally assume an idealized lattice. Varying pressure or temperature affects both the mobility and the degree of ordering of oxygen defects in opposite ways: increasing pressure(temperature) diminishes(enhances) the mobility of oxygen but increases(reduces) the degree of oxygen ordering [3]. Combined pressure/temperature experiments thus allow one to obtain information on relaxation phenomena in HTSC which could otherwise not be obtained.

Almost all previous studies of pressure-induced relaxation behavior in oxide superconductors have been restricted to the pressure range below 1 GPa where T_c normally increases linearly with pressure at a rate which may depend strongly on the temperature at which the pressure is changed [1, 7]. In strongly underdoped Y-123, for example, Fietz et al. [2] have shown that the derivative dT_c/dP increases tenfold if the pressure is changed at room temperature (RT) rather than at low temperatures (LT) below 90 K. Since for this system the relaxation processes appear to only become activated for temperatures above 240 K [3], the LT derivative $(dT_c/dP)_{LT}$ should reflect the initial pressure dependence of T_c, devoid of any relaxation effects. For the most underdoped Y-123 samples ($x \approx 6.4$), Fietz et al. find $(dT_c/dP)_{LT} \approx +2$ K/GPa, increasing with oxygen content x to a maximum value of +7 K/GPa for $x \approx 6.7$, before falling toward zero for nearly optimally doped samples [2]. It would be of interest to extend these previous measurements to 1 GPa to much higher pressures in order to obtain the intrinsic pressure dependence $T_c(P)$, free from relaxation effects. With the exception of our work on a single Y-123 sample [8], all previous *very*

high pressure studies on HTSC [1, 9] have been carried out by changing the pressure at RT, so that the measured $T_c(P)$ dependences may contain important contributions from relaxation effects.

In this paper we present the first hydrostatic high-pressure studies to 17 GPa on $YBa_2Cu_3O_x$ over the full range of oxygen content x where the temperature is maintained below 200 K to suppress relaxation effects. $T_c(P)$ follows a bell-shaped curve; both the initial slope dT_c/dP and the pressure $P(T_c^{\max})$ where $T_c(P)$ passes through a maximum take on their maximum values near $x \approx 6.7$. From the measurement of the pressure-dependent relaxation processes the activation volume for oxygen diffusion is found to be somewhat less than the molar volume of the O^{2-} ion and agrees within a factor of two with estimates from a simple hard-sphere diffusion model.

2 Experiment

The samples studied in the present experiments are single crystals of $YBa_2Cu_3O_x$ which have been broken off from the mother crystal. The crystals are grown in gold crucibles using the conventional "self-flux" procedure from a mixture containing Y:Ba:Cu in the ratios 5:27:68 using cooling rates varying from 0.3 to 1 °C/hour. The oxygen stoichiometries were subsequently adjusted by heating the crystals either in flowing O_2 or in a gas mixture of O_2 and N_2 as specified in Table 1. During the heat treatment, the oxygen pressure was continuously monitored using a zirconia-cell oxygen pressure monitor manufactured by Ametek, Inc. After the equilibration, the samples were quenched into liquid nitrogen to fix the stoichiometry. To obtain an equilibrium oxygen vacancy ordered condition at RT, the samples were aged at 295 K for over two months before measurements were performed. Stoichiometries were estimated using the calibration of stoichiometry vs. PO_2 (at 520°C) reported in Ref. [11].

The diamond-anvil cell (DAC), which is suitable for studies to very high pressures, is made of hardened copper-beryllium alloy fitted with 1/6-carat 16-sided diamond anvils having 0.5 mm culet diameter. Gaskets of Ni + 25 wt.% Mo alloy with diameter 2.2 mm and thickness near 300 μm are preindented to ~ 80 μm. The Y-123 crystal (typical size $0.1\times0.1\times0.05$ mm^3) together with a small ruby chip are placed in a 240 μm dia. hole drilled through the center of the gasket. The pressure clamp is placed in a continuous flow cryostat and superfluid ^{4}He is loaded into the gasket hole at 2 K to serve as pressure medium. The pressure in the gasket hole can be increased at any temperature at or below ambient by loading a membrane with a few bars of He gas to force the diamond-anvils together. The pressure in the cell can be determined at any temperature below RT by measuring the pressure-induced shift in the R1 fluorescence line of ruby. A second ruby chip at ambient pressure is located just outside the pressure cell, allowing the correction for the temperature shift of the ruby line. The superconducting transition of the Y-123 crystal is determined inductively to $\pm$ 0.3 K using a balanced primary/secondary coil system connected to

a PAR 124A lock-in amplifier by slowly varying the temperature (0.3 - 0.5 K/min.) through the transition. The ac susceptibility studies were carried out in 2 - 5 Oe (rms) magnetic fields at 1000 Hz.

The He-gas pressure system (Harwood) used is capable of generating hydrostatic pressures to 1.4 GPa. The CuBe pressure cell (Unipress) is inserted into a two-stage closed-cycle refrigerator (Leybold) which operates in the temperature range 2 - 320 K. The pressure in the cell is measured by a calibrated manganin gauge and can be changed at any temperature above the melting curve of the He pressure medium [10]. The superconducting transition of the Y-123 sample (typical size $1\times1\times0.15$ mm^3) in the high pressure environment is measured to $\pm$ 0.05 K accuracy by the ac susceptibility technique using a miniature primary/secondary coil system located inside the 7 mm I.D. bore of the pressure cell. In the present studies a magnetic field of 1.1 Oe (rms) at 507 Hz is applied along the short dimension of the sample ($H\|$ c-axis). Further details of the experimental setups for the diamond-anvil cell and He-gas systems are given elsewhere [12].

3 Results of Experiment and Discussion

3.1 Intrinsic Dependence of T_c on Pressure

The data in Fig. 1 on $YBa_2Cu_3O_{6.41}$ (sample B) serve to illustrate the dramatic effect that relaxation phenomena can have on $T_c(P)$: the pressure dependence of the transition temperature is seen to depend strongly on the *temperature* at which the pressure is changed! The initial slope dT_c/dP determined in a separate He-gas experiment to 0.8 GPa to high accuracy (straight lines in Fig. 1) increases almost tenfold if the pressure is changed at ambient, rather than low, temperature. In the DAC data to 13 GPa, T_c increases monotonically from 17 to 45 K if the pressure is applied at RT, but passes through a maximum near 23 K at 4 GPa if the sample is maintained at temperatures below 200 K throughout the entire experiment.

In the latter LT experiment $T_c(P)$ changes reversibly with pressure. However, as we discuss in more detail in the next subsection, relaxation effects lead to irreversibilities in $T_c(P)$ if the pressure is changed at RT. In general, $T_c(P)$ will depend on the entire pressure/temperature/time history of the sample. We thus write the measured transition temperature as the sum of two terms

$$T_c(x,P,T,t) = T_c^{intrin}(x,P) + \Delta T_c^{relax}(x,P,T,t), \qquad (1)$$

a reversible "intrinsic" pressure dependence obtained by holding the sample at a sufficiently low temperature during the entire experiment, plus a temperature- and time-dependent correction term to take into account the effects of relaxation. The intrinsic dependence $T_c^{intrin}(P)$ most directly reflects the dependence of T_c on pressure-induced changes in the basic solid state properties, including the pairing interaction itself, and thus should be of most value in comparison with theory.

In Fig. 2 we plot $T_c(P)$ to 17 GPa for sample B from Fig. 1 and for four further $YBa_2Cu_3O_x$ crystals with varying oxygen content x covering the entire underdoped to optimally doped range; throughout these experiments the samples were maintained at temperatures below 200 K. The straight lines give the initial slopes from the corresponding He-gas studies to 0.8 GPa and are seen to match up well with the DAC data; these slopes are listed under $(dT_c/dP)_{LT}$ in Table 2. As outlined below, in the He-gas data no evidence for relaxation effects in T_c was found in the temperature range between T_c and 200 K (the measurement of T_c involves passing the sample through temperatures near T_c over a one hour period, so that the time-dependence of relaxation processes activated at temperatures below T_c cannot be studied). Unless there are, in fact, such very low temperature relaxation effects below T_c, the pressure dependences $T_c(P)$ in Fig. 2 and $(dT_c/dP)_{LT}$ in Table 2 do indeed represent the intrinsic dependence of T_c on pressure for the $YBa_2Cu_3O_x$ system.

The initial slope $(dT_c/dP)_{LT}$ in Fig. 2 and Table 2 is seen to increase gradually with oxygen content A→B→C, reaching a particularly large value (+7.1 K/GPa) for sample D and then decreasing sharply to +0.24 K/GPa for the nearly optimally doped sample E. This dependence of the initial slope on oxygen content x agrees well with the results of earlier He-gas experiments by Fietz et al. [2] which were carried out at temperatures below 90 K. In these latter data $(dT_c/dP)_{LT}$ versus x peaks sharply at $x = 6.66$. This peak is presumably related to the transition from the ortho-I to ortho-II phase [13], and higher order superstructures [14], in this compound near this value of x . It is interesting to note that similar results are found for superconducting $PrBa_2Cu_3O_x$, giving evidence that the origin of superconductivity in both systems is the same [15].

For the data in Figs. 1 and 2 it is seen that the *pressure* where $T_c(P)$ passes through its maximum appears to be directly correlated with the *magnitude* of the initial slope $(dT_c/dP)_{LT}$: if one increases, so does the other. This holds even though the initial slope in Fig. 2 changes in a markedly nonmonotonic fashion with oxygen content x. We now attempt to account for this and other features of the $T_c(P)$ data in Fig. 2.

In high-T_c superconductors the dependence of T_c on the carrier concentration n is believed to follow an approximate inverted parabolic dependence [16],

$$T_c(n) \simeq T_c^{\max}\left[1 - A(n - n_{opt})^2\right], \tag{2}$$

where $T_c^{\max}, A$, n and n_{opt} all may be functions of pressure. In $YBa_2Cu_3O_x$ the carrier concentration n can be varied by changing the oxygen concentration x, by cation substitution or by applying pressure. Hall effect studies on a variety of HTSC systems [17], including Y-123, reveal that under pressure hole charge is transferred into the CuO_2 planes at a typical rate $d\ln n/dP \approx +10\%$/GPa. In the "simple charge-transfer model" [1], the dependence of T_c on pressure arises solely from the increase in n in Eq. 2, all other parameters remaining constant. This simple model leads to the following expectations: (1) $T_c(P)$ should follow an inverted parabolic

dependence, initially increasing with pressure for an underdoped sample, passing through a maximum and then decreasing to zero; (2) for underdoped samples, the higher the oxygen content, the lower the initial slope $(dT_c/dP)_{LT}$ and the smaller the pressure needed to reach the maximum value of $T_c(P)$; (3) the maximum value of $T_c(P)$ should be independent of the initial oxygen content; (4) for optimally doped samples, where $n = n_{opt}$, the initial slope $(dT_c/dP)_{LT}$ should be zero; for overdoped samples, $T_c(P)$ should decrease monotonically to zero under pressure. All these expectations from the simple charge-transfer model are inconsistent with the data in Fig. 2. In particular, for Y-123 and many other optimally doped HTSC, the initial slope is not zero, but positive, $(dT_c/dP)_{LT} \approx +1$ to $+2$ K/GPa [18].

Neumeier and Zimmermann [19] have carried out a successful analysis of high-pressure data on a series of cation substituted Y-123 compounds in terms of a *modified* charge-transfer model based on Eq. 2 which breaks the total pressure derivative of T_c up into two parts:

$$\left(\frac{dT_c}{dP}\right) = \left(\frac{\partial T_c}{\partial n}\right)\left(\frac{\partial n}{\partial P}\right) + \left(\frac{dT_c}{dP}\right)_{noCT}. \qquad (3)$$

The first term on the right side of this equation takes into account the effect on T_c of the normal transfer of hole charge *into* the CuO_2 plane(s) with increasing pressure [1, 20] (i.e. $\partial n/\partial P > 0$) whereas the second term gives the "no charge transfer" contribution to the pressure dependence of T_c which arises from changes in $T_c^{\max}$, A, and n_{opt} under pressure (see Eq. 2). An explicit relation between the pressure derivative of these parameters and $(dT_c/dP)_{noCT}$ can be obtained by taking the total pressure derivative of Eq. 2 and setting it equal to Eq. 3. From an analysis of their data on the *nearly optimally doped* Y-123 compounds, Neumeier and Zimmermann [19] were able to fit their $T_c(P)$-data if $(dT_c/dP)_{noCT} \approx +1$ K/GPa and $\partial n/\partial P \approx +0.011$ holes/GPa; the value of $\partial T_c/\partial n$ in Eq. 3 is taken from Ref. [16]. This model is able to account for the universal positive pressure derivative dT_c/dP for optimally doped samples, but it is not able to give quantitative agreement with "intrinsic" $T_c(P)$-data over a wide doping range, as seen in a recent study on Hg-1201 [21]. The addition of a constant $(dT_c/dP)_{noCT}$ term in Eq. 3, together with Eq. 2, leads to the expectation that for strongly underdoped superconductors T_c should reach a value well above that for optimal doping (93 K), contrary to experiment. This model also leads to the same conclusions (1) and (2) as above in the simple charge-transfer model, contrary to the present experiments.

The inability of the modified charge-transfer model to account for the present results on Y-123 may arise in part from a dependence of the contribution $(dT_c/dP)_{noCT}$ on oxygen content, but is certainly also due to the fact that the measured dependence of T_c on x does not follow an inverse parabolic dependence, as one would expect from Eq. 2 if n were proportional to x, but rather exhibits a marked plateau near $x = 6.6$ which arises from the well known ortho-I to ortho-II transition in the oxygen sublattice [13]. The concentration of hole charge carriers n in the CuO_2 plane(s) depends

not only on the concentration of oxygen defects, but also on how they arrange themselves within the basal plane. In this system, therefore, one should not be surprised if n is a markedly nonlinear function of x.

It is a puzzling result indeed that $(dT_c/dP)_{LT}$ versus x shows a peak at $x \simeq 6.66$ [2] since at low temperatures the lack of relaxation phenomena appears to imply that the distribution of oxygen defects does not change with pressure. Apparently the rate of pressure-induced charge flow into the CuO_2 planes is a sensitive function of the distribution of oxygen defects, even if they are frozen in place at LT and do not move around as pressure is applied. There is also the possibility that for samples with oxygen content near $x \simeq 6.7$, where $T_c \approx 65$ K, changing the pressure activates fast relaxation processes which cannot be detected in the present experiments because they occur on a too rapid time scale for temperatures near $T_c \simeq 65$ K. LT relaxation was indeed observed for Tl-2201 at temperatures as low as 15 K. Previous studies on a strongly underdoped Y-123 crystal with $T_c(0) \simeq 17$ K, however, failed to reveal any sign of LT relaxation. This does not prove that the 65K-sample is devoid of LT relaxation since it contains almost twice as many oxygen defects which might open new avenues for defect relaxation. The issue of fast relaxation in Y-123 will be further discussed in the next section. We thus see that even the intrinsic $T_c(P)$-data for Y-123 free of relaxation effects are quite complex. At the present time we are unable to offer a quantitative analysis of these data.

3.2 Relaxation Effects in T_c

We now discuss in detail the relaxation data for samples B - E in comparison to our published data for sample A [3]. The relaxation measurements on samples B and C were particularly extensive; typical results are shown in Figs. 3, 4 and 5 and listed in Table 2.

We first consider the results for sample B where $T_c(1 \text{ bar}) \simeq 17.1$ K (pt. 1 in Fig. 3). Following the application and retention of 0.65 GPa pressure at 298 K for 1 hour, the sample was cooled in 2 hours to LT and T_c measured (pt. 2) [22]. The sample was then warmed back up to 298 K and annealed at that temperature for varying lengths of time up to 176 hours total, as seen in Figs. 3 and 4(a) (pts. 3-9) . The pressure was then reduced to 0.41 GPa at 62 K (pt. 10) and then to 0.26 GPa (pt. 11), and the relaxation in $T_c(t)$ determined for consecutively longer annealing times at 298 K to 79 hours total (pts. 11-18 in Figs. 3 and 4(b)). Finally, the pressure was released to 0.13 GPa at 45 K (pt. 19) and then to 1 bar and $T_c(t)$ determined for annealing at 303 K (pts. 20-25 in Figs. 3 and 4(c)); as discussed below, including the higher annealing temperature allows an estimate of τ_o in the Arrhenius law. T_c for pt. 25 is seen to almost fully relax back to its initial value at ambient pressure.

For sample B the average pressure derivative of T_c for pressure changes at low temperatures is $(dT_c/dP)_{LT} \simeq +2.1$ K/GPa, as listed in Table 2. On the other hand, for pressure changes at RT a much larger value $(dT_c/dP)_{RT} \simeq +19.5$ K/GPa is

obtained if the sample is annealed at 298 K for sufficient time (> 150 hours) to allow full relaxation (slope between pts. 1 and 9 in Fig. 3). The LT and RT derivatives are given in Table 2 for all samples. If we define the total measured pressure derivative at RT to be the sum of intrinsic and relaxation (oxygen-ordering) contributions

$$\left(\frac{dT_c}{dP}\right)_{RT} \equiv \left(\frac{dT_c}{dP}\right)_{intrin} + \left(\frac{dT_c}{dP}\right)_{relax}, \tag{4}$$

then, assuming that $(dT_c/dP)_{intrin} \simeq (dT_c/dP)_{LT}$, we see that for sample B the relaxation contribution $(dT_c/dP)_{relax} \simeq +17.4$ K/GPa dominates ($8\times$) over the intrinsic contribution. Four further sets of relaxation data were taken at various temperatures and pressures on sample B to allow a more complete analysis [23].

Sample C was mounted in the pressure cell together with sample B, so relaxation data were obtained under identical conditions, as seen in Fig. 5. From the release of pressure at LT the intrinsic pressure derivative is determined to be $(dT_c/dP)_{LT} \simeq +2.25$ K/GPa, whereas the RT derivative is $(dT_c/dP)_{RT} \simeq +12.6$ K/GPa, yielding from Eq. 4 the relaxation derivative $(dT_c/dP)_{relax} \simeq +10.3$ K/GPa, almost five times the value of the intrinsic derivative.

The effect of relaxation processes on the measured pressure dependence $T_c(P)$ is illustrated in Fig. 6 for $YBa_2Cu_3O_{6.66}$ (sample D) where $T_c(1\,\text{bar}) \simeq 64.2$ K. Applying and holding 0.79 GPa pressure at RT for 2 hours results in a strong increase in T_c with slope $(dT_c/dP)_{RT} \simeq +9.28 \pm 0.15$ K/GPa [24]. If the pressure is released at LT (~ 60 K), T_c is seen to decrease with a lesser slope $(dT_c/dP)_{LT} \simeq +7.14 \pm 0.20$ K/GPa, taking on a value (pt. 4) at ambient pressure ~ 1.5 K higher than its initial value (pt. 1). Annealing sample D then for 1 hour at 100 K (pt. 5) and then 200 K (pt. 6) causes no relaxation in T_c. Only if the sample is annealed for 1 hour at 298 K does T_c relax back fully (pt. 7) to its initial value (pt. 1). As seen in Table 2, the relaxation effects for sample D are much smaller than for samples A, B, or C.

Sample E does not show any relaxation behavior in T_c; we find the pressure derivatives $(dT_c/dP)_{RT} = (dT_c/dP)_{LT} \simeq +0.24$ K/GPa. The absence of relaxation in T_c presumably arises from two effects: (1) The oxygen content $x \simeq 6.92$ is near the stoichiometric value $x \simeq 7.0$ so there are only few oxygen vacancies in the chain sites to order. (2) Oxygen ordering is believed to change T_c solely through the charge transfer Δn it causes [25]; any residual oxygen ordering effects which might occur should cause negligible change in T_c since for an optimally doped sample $\partial T_c/\partial n = 0$ in Eq. 3. We note that the values for the LT and RT pressure derivatives of T_c for samples A - E listed in Table 2 are in reasonably good agreement with the extensive He-gas data of Fietz et al. [2] on the Y-123 system.

We now attempt to fit the above time-dependent relaxation data $T_c(t)$ for samples A -C using the stretched-exponent expression [26]

$$T_c(t) = T_c(\infty) - [T_c(\infty) - T_c(0)] \exp\left\{-\left(\frac{t}{\tau}\right)^{\alpha}\right\}, \tag{5}$$

where τ is the temperature-dependent relaxation time which is related to the activation energy barrier E_A by the Arrhenius law

$$\tau(T,P) = \tau_o \exp\left\{\frac{E_A(T,P)}{k_B T}\right\}, \tag{6}$$

and τ_o is the attempt period. The results of the best fits using Eq. 5 for samples B and C are given by the solid lines through the data in Figs. 4 and 5, yielding the values of the relaxation time τ given in the figures. In these fits the stretched exponent was fixed at the value $\alpha = 0.6$; this value $\pm$ 0.08 was found to give the best fit both in the present (samples B and C) and earlier studies (sample A) [3].

In Fig. 7 we plot the values of τ at ambient and 0.65 GPa pressures versus the inverse temperature. We see that, within experimental error, the value of the attempt period $\tau_o \approx 1.4 \times 10^{-12}$ s obtained from temperature-quench experiments on Y-123 [27] fits both the ambient and high pressure data (solid lines); an accurate determination of $d\tau_o/dP$ would require more exhaustive data over a much wider temperature range. However, one can argue on general grounds that the pressure dependence of τ_o should be small [28].

3.3 Relaxation Effects in the Electrical Resistivity

Since charge transfer to or from the conducting CuO_2 plane(s) is responsible for the relaxation behavior in T_c [25], the normal-state electrical resistivity $\rho(t)$ should also change. Using the electrical resistivity rather than T_c to monitor the degree of relaxation has a number of advantages: (1) the entire experiment can be carried out at a constant temperature, (2) the relaxation can be measured immediately following pressure changes, and (3) many more data points can be readily obtained.

Sample C was first held at a constant temperature of 298 K for 40 hours to allow the oxygen defect distribution to reach equilibrium at this temperature. Then 0.70 GPa pressure was applied over a 10 minute period, resulting in a resistivity drop by 0.8 mΩcm from 14.1 to 13.3 mΩcm at 298 K; the time-dependent resistivity at this temperature was then measured for a total of 120 hours, as seen in Fig. 8(a). For clarity, only 2% of all measured data points are shown. Over the 120 hour period, the resistivity decreased by approximately 2 mΩcm. After the relaxation under 0.70 GPa pressure was almost complete, the pressure was reduced to 0.34 GPa, maintaining the temperature at 298 K. This decrease in pressure resulted in an instantaneous resistivity increase of 0.30 mΩcm. The relaxation $\rho(t)$ was then measured as a function of time for 95 hours at 298 K, as seen in Fig. 8(b), resulting in a further resistivity increase of 0.65 mΩcm. The pressure was then fully released at 298 K, causing the resistivity to increase instantly by 0.35 mΩcm, and the time-dependent relaxation measured for 170 hours, whereby $\rho(t)$ increased by a further 1.45 mΩcm. The final value $\rho(298\ \mathrm{K}) \simeq 14.1$ mΩcm agrees exactly with the initial value, confirming the reversibility of the observed relaxation effects. A second experiment

was carried out on sample C where 0.35 GPa pressure was applied from ambient and the relaxation in the resistivity $\rho(t)$ determined. The relaxation in $\rho(t)$ was also studied for sample D at 298 K at pressures 0.70 GPa and 1 bar. The experimental results are analyzed below and the parameters obtained listed in Tables 2 and 3.

The time dependences of the relaxation measurements using the normal state resistivity are seen to be similar to those observed in the measurements of $T_c(t)$ described above. We analyze the time-dependent resistivity data $\rho(t)$ at 298 K using a stretched exponent expression analogous to that used for $T_c(t)$ in Eq. 5, namely

$$\rho(t) = \rho(\infty) - [\rho(\infty) - \rho(0)] \exp\left\{-\left(\frac{t}{\tau}\right)^{\alpha}\right\}, \tag{7}$$

where $\rho(\infty)$ and $\rho(0)$ are the resistivities of the sample at infinite time and before any relaxation takes place, respectively. The fit to the resistivity data should give much more accurate results since several thousand data points were obtained during each run. The results of the fits to the resistivity relaxation data using Eq. 7 are listed in Table 3 for samples C and D, including the values of the activation energy E_A calculated from τ using Eq. 6. As before with the $T_c(t)$ relaxation data, we fix the value of the stretched exponent at $\alpha = 0.6$. For sample C the quality of the $\rho(t)$ data allows us to use α as a fit parameter; the values of α giving the best fits are listed in Table 3 and Fig. 8 along with other fit parameters. The quality of the fits using both values of α is indistinguishable on the scale of the graph in Fig. 8. The pressure dependence of the activation energy dE_A/dP listed in Table 2 is, within experimental error, independent of the value of α used.

The pressure dependence of the activation energy $E_A(P)$ obtained from the fits is plotted in Fig. 9 for samples A - D using both $T_c(t)$ and $\rho(t)$ to probe the degree of relaxation. In our previous study on sample A [3], E_A was found to increase linearly with pressure to 2.3 GPa. A linear least-squares fit to the data in Fig. 9 results in the values of the slope dE_A/dP given in Table 2 [29].

The pressure dependence of relaxation effects is usually analyzed in terms of the activation volume ΔV_A which can be calculated from the pressure dependence of the activation energy [30]

$$\Delta V_A = \Delta V_f + \Delta V_m = N_A \left(\frac{dE_A}{dP}\right), \tag{8}$$

where N_A is Avogadro's number and ΔV_f and ΔV_m are the formation and migration volumes per mol, respectively. The activation volumes calculated from Eq. 8 are given in Table 2. We compare these activation volumes with the molar volume of the diffusing species $V_{O^{2-}} \simeq 5.78$ cm^3/mol [31].

Since here the relaxation behavior is believed to arise from oxygen defects in the basal plane which were introduced during the synthesis, and thus need not be formed through the application of pressure, the formation volume should be zero. The measured activation volume should thus correspond solely to the migration volume.

Unfortunately, to our knowledge there are no theoretical estimates of the migration volume for the high-T_c oxides. We have recently applied a simple, hard-sphere approach to estimate ΔV_m where we assume that the diffusing oxygen defect in the basal plane first moves from the O(1) site of one chain fragment to the adjacent O(5) site and then back to a parallel chain site [23, 32]. The results of the hard-sphere model are that $\Delta V_m \approx +1.9$ cm^3/mol for samples A, B, and C, whereas $\Delta V_m \approx +2.0$ cm^3/mol for sample D. These values are approximately half as large as the experimental results for the activation volume in Table 2. In simple bcc and fcc crystals the hard-sphere model generally overestimates the experimental values by a factor of 2 or 3 [33]. Since the superconducting oxides in consideration here are not closely packed, but fairly open structures, it is reasonable to expect that estimates from the hard-sphere model would be lower than the experimental values [34]. In the hard-sphere model, all non nearest-neighbor interactions are neglected; in ionic compounds, like the high-T_c superconductors, long-range Coulomb interactions are important and will certainly make an important contribution to the migration volume.

Acknowledgments

The work at Washington University is supported by the National Science Foundation under grant DMR 98-03820. Work at Argonne was supported by the U.S. Department of Energy, Division of Basic Energy Sciences, under Contract No. W-31-109-ENG-38.

References

[1] See: J. S. Schilling and S. Klotz, in: *Physical Properties of High Temperature Superconductors*, Vol. III, ed. D. M. Ginsberg (World Scientific, Singapore, 1992) p. 59, and references therein.

[2] W. H. Fietz, R. Quenzel, H. A. Ludwig, K. Grube, S. I. Schlachter, F. W. Hornung, T. Wolf, A. Erb, M. Kläser, and G. Müller-Vogt, Physica C 270, 258 (1996).

[3] S. Sadewasser, Y. Wang, J. S. Schilling, H. Zheng, A. P. Paulikas, and B. W. Veal, Phys. Rev. B 56, 14168 (1997).

[4] R. Sieburger and J.S. Schilling, Physica C 173, 423 (1991).

[5] A.-K. Klehe, C. Looney, J. S. Schilling, H. Takahashi, N. Môri, Y. Shimakawa, Y. Kubo, T. Manako, S. Doyle, A. M. Hermann, Physica C 257, 105 (1996).

[6] C. Looney, J. S. Schilling, S. Doyle, A. M. Hermann, Physica C 289, 203 (1997).

[7] J.S. Schilling, C. Looney, S. Sadewasser, and Y. Wang, Rev. High Pressure Sci. Technol. 7, 425 (1998).

[8] V.G. Tissen, Y. Wang, A.P. Paulikas, B.W. Veal, and J.S. Schilling, Physica C 316, 21 (1999).

[9] H. Takahashi and N. Mori, in: *Studies of High Temperature Superconductors,* Vol. 16/17, ed. A.V. Narlikar (Nova Science Publishers, Inc., N.Y., 1995) p. 1.

[10] I. L. Spain and S. Segall, Cryogenics 11, 26 (1971).

[11] J. D. Jorgensen, B. W. Veal, A. P. Paulikas, L. J. Nowicki, G. W. Crabtree, H. Claus, and W. K. Kwok, Phys. Rev. B 41, 1863 (1990).

[12] J. S. Schilling, J. Diederichs, S. Klotz and R. Sieburger in: *Magnetic Susceptibility of Superconductors and Other Spin Systems*, eds. R. A. Hein, T. L. Francavilla and D. H. Liebenberg (Plenum, New York, 1991) p. 107.

[13] See, for example, R. Beyers and T. M. Shaw, in: *Solid State Physics Vol. 42,* edited by H. Ehrenreich and D. Turnbull (Academic Press, Inc., N.Y., 1989) p. 135.

[14] M. v. Zimmermann, T. Frello, N. H. Andersen, J. Madsen, M. Käll, O. Schmidt, T. Niemöller, J. R. Schneider, H. F. Poulsen, Th. Wolf, R. Liang, P. Dosanjh, W. N. Hardy (preprint).

[15] J. Ye, S. Sadewasser, J. S. Schilling, Z. Zou, A. Matsushita, and T. Matsumoto (submitted for publication).

[16] M. R. Presland, J. L. Tallon, R. G. Buckley, R. S. Liu, and N. D. Flower, Physica C 176, 95 (1991).

[17] C. Murayama, Y. Iye, T. Enomoto, N. Môri, Y. Yamada, T. Matsumoto, Y. Kubo, Y. Shimakawa, and T. Manako, Physica C 183, 277 (1991).

[18] A.-K. Klehe, A. K. Gangopadhyay, J. Diederichs, and J. S. Schilling, Physica C 213, 266 (1993).

[19] J. J. Neumeier and H. A. Zimmermann, Phys. Rev. B 47, 8385 (1993).

[20] O. Chmaissem, J. D. Jorgensen, S. Short, A. Knizhnik, Y. Eckstein, H. Shaked, Nature 397, 45 (1999).

[21] S. Sadewaser, J. S. Schilling, J. L. Wagner, O. Chmaissem, J. D. Jorgensen, D. G. Hinks, and B. Dabrowski, Phys. Rev. B 60 (Oct. 1, 1999).

[22] The T_c-values for point 2 in Figs. 4(a) and 5(a) contains some effects of relaxation since the 0.65 GPa pressure was applied at RT in 10 minutes and held for one hour before cooling down in two hours to LT to measure T_c. The asterisked (*) points in Figs. 4(a) and 5(a) are our estimate of the $T_c(t = 0)$ values at this pressure had no relaxation occurred; the procedure used for this estimate is described in detail in Ref. [3]. All data is then used to calculate the relaxation time τ from a fit to Eq. 5 setting $\alpha = 0.6$.

[23] S. Sadewasser (Ph.D. Thesis, Washington University, August 1999).

[24] Due to the contraction of the He pressure medium upon cooling, the pressure at temperatures near T_c is reduced to 0.68 GPa, a value 0.11 GPa lower than at RT. Since for sample D the "intrinsic" pressure dependence of T_c dominates over that from relaxation effects, it is more appropriate to use the value of the pressure at LT to calculate $(dT_c/dP)_{RT}$. This procedure is also appropriate for sample E which exhibits no relaxation effect in T_c. However, for samples A - C, where the relaxation effects dominate over the intrinsic, and most of the relaxation takes place at temperatures near RT, it is better to use the value of the pressure at RT when calculating $(dT_c/dP)_{RT}$. Obviously, to calculate $(dT_c/dP)_{LT}$ the value of the pressure at LT is correct.

[25] H. Takahashi, A.-K. Klehe, C. Looney, J. S. Schilling, N. Môri, Y. Shimakawa, Y. Kubo and T. Manako, Physica C 217, 163 (1993).

[26] R. G. Palmer, D. L. Stein, E. Abrahams, and P. W. Anderson, Phys. Rev. Lett. 53, 958 (1984); D. Redfield, in *Amorphous Silicon Technology - 1992,* edited by M. J. Thompson et al., MRS symposia Proceedings No. 258 (Materials Research Society, Pittsburgh, 1992), p. 341.

[27] B. W. Veal, A.P. Paulikas, H. You, H. Shi, Y. Fang, and J. W. Downey, Phys. Rev. B 42, 6305 (1990).

[28] Since the attempt frequency is presumably of the order of a typical phonon frequency, the pressure dependence of τ_o can be estimated from the Grüneisen relation $\gamma = -\partial \ln \omega / \partial \ln V \simeq \partial \ln \tau_o / \partial \ln V$, where V is the volume, ω is a phonon frequency and a typical value for the Grüneisen parameter is $\gamma \simeq 2$. With a typical relative volume change of $\Delta V/V \approx 1\%$/GPa for high-T_c superconductors [1], the relative change of the attempt period τ_o under 1 GPa pressure would be $\Delta\tau_o/\tau_o \simeq 2\Delta V/V \simeq 2\%$. This change in τ_o by 2% is negligible compared to the change in the relaxation time τ for 1 GPa which is $\sim 550\%$ from the above data.

[29] The initial measurement of the relaxation in T_c for samples B and C was carried out at 0.12 GPa, followed by the full release of pressure. More extensive measurements of the relaxation were then carried out to higher pressures, revealing an approximate linear dependence of E_A on pressure. The measurement at 0.12

GPa was omitted from the linear least-squares fits in Fig. 9. The reason for the deviation of the 0.12 GPa point is not understood.

[30] G. W. Tichelaar and D. Lazarus, Phys. Rev. 113, 438 (1959).

[31] D. R. Lide, *Handbook of Chemistry and Physics,* 71st edition, (CRC Press, Inc., 1990) p. 12-1.

[32] S. Sadewasser, J. S. Schilling, and A. M. Hermann (in preparation).

[33] D. Lazarus and N. H. Nachtrieb, in *Solids under Pressure,* edited by W. Paul and D. M. Warschauer (McGraw Hill, N.Y., 1963), and references therein.

[34] Note that if the structure in the hard-sphere model is sufficiently loosely packed, the diffusing ion can proceed through the lattice without touching other ions, implying $\Delta V_m = 0$ which is clearly an underestimate.

TABLES

Table 1. Heat treatment given single crystalline $YBa_2Cu_3O_x$ samples with oxygen stoichiometry x. T_c values at ambient pressure are also listed.

sample	x	T_c(K)	heat treatment
A	6.41	13.5	309 h @ 520°C in 0.113% O_2/N_2
B	6.41	17.1	234 h @ 520°C in 0.100% O_2/N_2
C	6.45	34.4	475 h @ 520°C in 0.191% O_2/N_2
D	6.66	64.2	282 h @ 520°C in 4% O_2/N_2
E	6.95	92.5	5 days @ 480°C plus 7 days @ 420°C in O_2

Table 2. The initial pressure derivatives of T_c and the results of the relaxation studies on $YBa_2Cu_3O_x$ for samples B-E in the present studies and sample A from Ref. [3]. Values of $(dT_c/dP)_{RT}$ for samples A - C are for full relaxation $T_c(t \rightarrow \infty)$ following change of pressure. T_c for sample D was measured after annealing for only 2 hours after applying 0.79 GPa at 298 K. Results using T_c as monitor are given in first five rows; results from resistivity studies ρ are given in last two rows. Values of E_A at ambient pressure are estimated from fits to relaxation data using $\alpha = 0.6$. NM means "not measured" using indicated monitor; NR means "no relaxation" detected. The activation volume is calculated using Eq. 8.

sample	T_c(K)	$(dT_c/dP)_{RT}$ (K/GPa)	$(dT_c/dP)_{LT}$ (K/GPa)	E_A(eV)	dE_A/dP (eV/GPa)	ΔV_A (cm^3/mol)
A-T_c	13.5	+20.1(1)	+2.0(1)	0.973(2)	+0.044(2)	+4.2(2)
B-T_c	17.1	+20(5)	+2.1(2)	0.977(1)	+0.029(3)	+2.8(3)
C-T_c	34.4	+13(3)	+2.3(1)	0.967(1)	+0.037(4)	+3.6(4)
D-T_c	64.2	+9.3(2)	+7.1(2)	NM	NM	NM
E-T_c	92.5	+0.24(6)	+0.24(6)	NR	NR	NR
C-ρ	NM	NM	NM	0.971(2)	+0.024(6)	+2.4(6)
D-ρ	NM	NM	NM	0.936(0)	+0.056(0)	+5.4(0)

Table 3. Parameters obtained from fits using Eq. 7 to resistivity data on $YBa_2Cu_3O_x$ (samples C and D). See text for details.

sample	P(GPa)	$\rho(\infty)$ mΩcm	$\rho(0)$ mΩcm	$\tau(h)$	α	E_A(eV)
C	0.70	11.17	13.44	20.99(1)	0.51	0.990
		11.28	13.29	20.77(3)	0.60	0.989
C	0.34	12.36	11.71	12.34(1)	0.62	0.976
		12.37	11.70	12.28(1)	0.60	0.976
C	0	14.16	12.71	12.03(1)	0.67	0.975
		14.17	12.47	9.96(2)	0.60	0.971
C	0.35	12.13	13.77	16.20(1)	0.54	0.983
		12.17	13.66	17.21(1)	0.60	0.985
C	0	14.09	12.56	12.21(0)	0.65	0.976
		14.10	12.42	11.03(1)	0.60	0.973
D	0.70	1.854	1.939	11.79(7)	0.60	0.975
D	0	2.122	2.042	2.59(2)	0.60	0.936

FIGURE CAPTIONS

Fig. 1. Dependence of T_c on hydrostatic pressure in DAC for $YBa_2Cu_3O_{6.41}$ (sample B) for increasing ($\bullet$, $\blacktriangle$) or decreasing ($\circ$, $\triangle$) pressure at 298 K or temperatures below 200 K. Straight solid lines give slope of corresponding He-gas data to 0.8 GPa. Dashed lines are guides to the eye.

Fig. 2. Dependence of T_c on hydrostatic pressure in DAC for $YBa_2Cu_3O_x$ with increasing oxygen content x (samples A-E) for increasing (closed symbols) or decreasing (open symbols) pressure at temperatures below 200 K. Data for sample A from Ref. [3]. Straight solid lines give slopes from He-gas studies to 0.8 GPa at low temperatures (see Table 2). Dashed lines are guides to the eye.

Fig. 3. Dependence of T_c on hydrostatic pressure in the He-gas system for $YBa_2Cu_3O_{6.41}$ (sample B) illustrating relaxation behavior. Numbers give order of measurement. Solid lines are guides to the eye.

Fig. 4. Relaxation behavior of T_c versus annealing time in the He-gas system for $YBa_2Cu_3O_{6.41}$ (sample B) under the conditions: annealing at 298 K following the (a) application of 0.65 GPa and the (b) reduction to 0.30 GPa; annealing at 303 K following pressure release to 1 bar. Numbers give order of measurements, matching those in Fig. 3. Meaning of asterisked (*) data point is discussed in Ref. [3]. Solid lines give results of fits using Eq. 5 setting $\alpha = 0.6$.

Fig. 5. Relaxation behavior of T_c versus annealing time in the He-gas system for $YBa_2Cu_3O_{6.45}$ (sample C) under the conditions: annealing at 298 K following the (a) application of 0.65 GPa and the (b) reduction to 0.30 GPa; annealing at 303 K following release to 1 bar. Numbers give order of measurements. Meaning of asterisked (*) data point is discussed in Ref. [3]. Solid lines give results of fits using Eq. 5 setting $\alpha = 0.6$.

Fig. 6. Dependence of T_c on hydrostatic pressure in the He-gas system for $YBa_2Cu_3O_{6.66}$ (sample D). Pressure is applied at 298 K but released at 60 K. Numbers give order of measurement. Straight lines are fits to data using values for the derivative dT_c/dP given in the figure and Table 2.

Fig. 7. Dependence of relaxation time τ on inverse temperature for $YBa_2Cu_3O_x$ (samples B and C) for both ambient and 0.65 GPa pressure. Solid line is fit to data with Eq. 6 using $\tau_o \simeq 1.4\times10^{-12}$ s [27]; the dashed line is least-squares fit.

Fig. 8. Relaxation behavior of the electrical resistivity ρ at 298 K versus time t for $YBa_2Cu_3O_{6.45}$ (sample C) in the He-gas system following (a) application of 0.70 GPa, (b) reduction of pressure to 0.34 GPa, (c) release of pressure to 1 bar. For clarity, only 2% of all data points are shown. Solid lines are fits to data using Eq. 7 with parameters given in the figure and Table 3.

Fig. 9. Dependence of the activation energy E_A on pressure for $YBa_2Cu_3O_x$ samples A - D using both T_c and ρ as relaxation monitors. Dashed lines are linear least-squares fits to data yielding values of slope dE_A/dP given in the figure and Table 2.

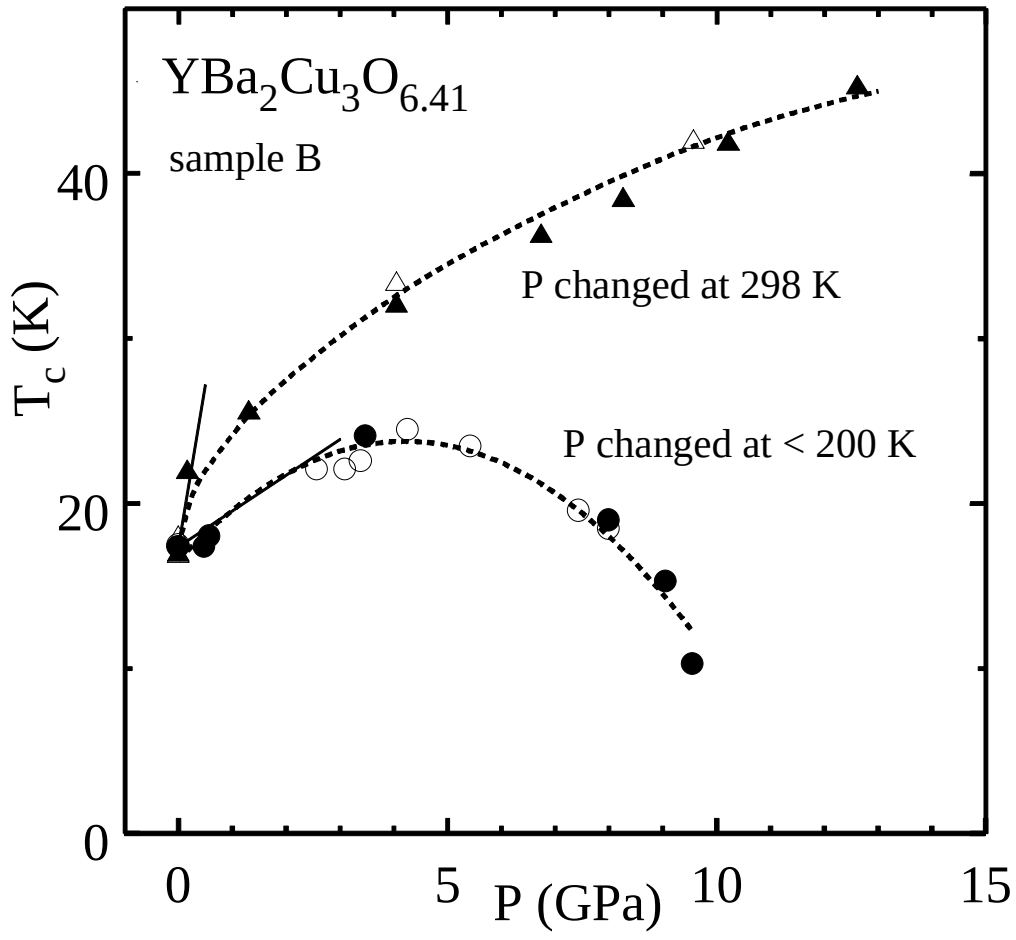
YBa2Cu3O6.41
sample B
P changed at 298 K
P changed at < 200 K
Tc (K)
P (GPa)
0
20
40
0
5
10
15

Figure 1:

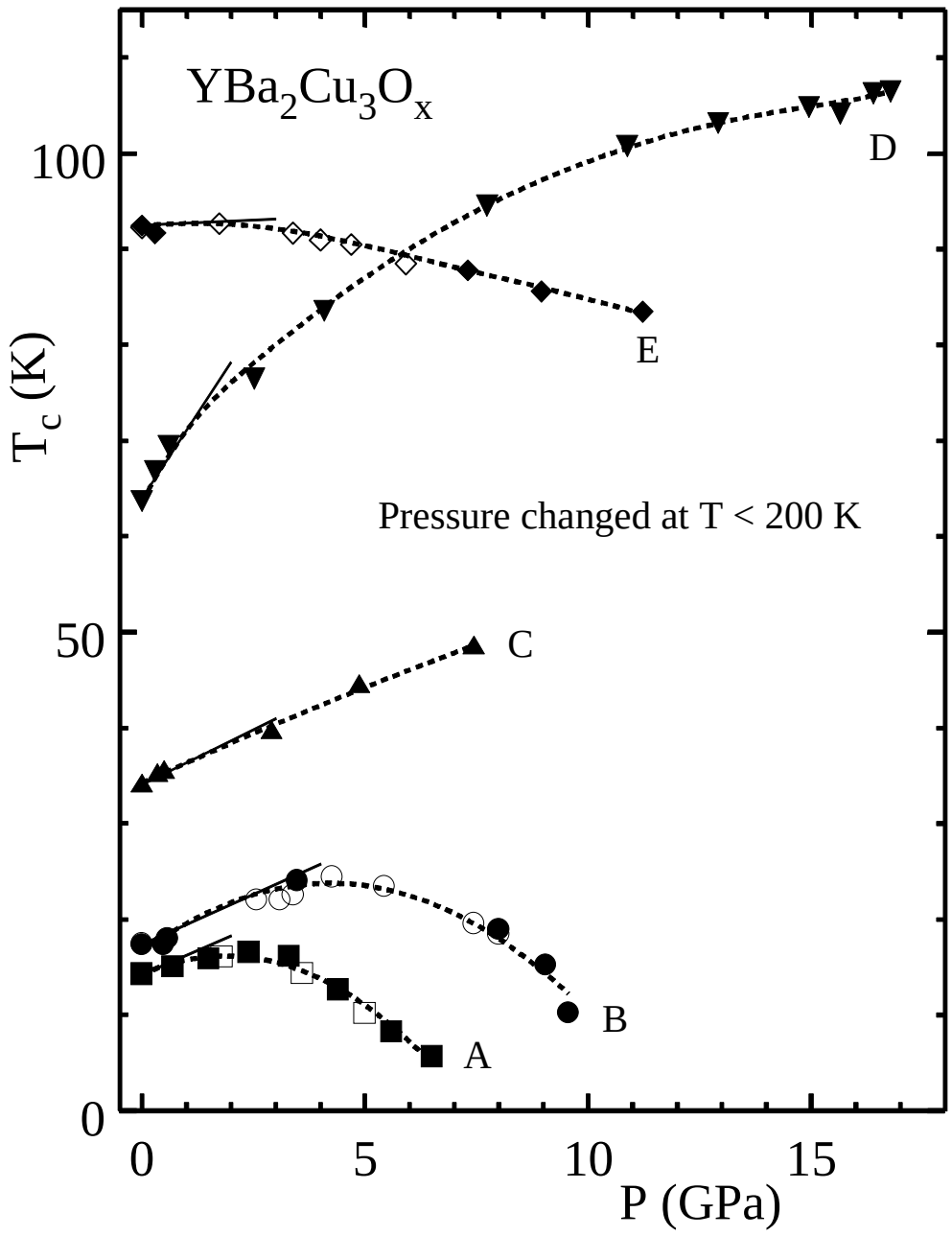
YBa2Cu3Ox
100
50
0
Tc (K)
0
5
10
15
P (GPa)
D
E
C
B
A
Pressure changed at T < 200 K

Figure 2:

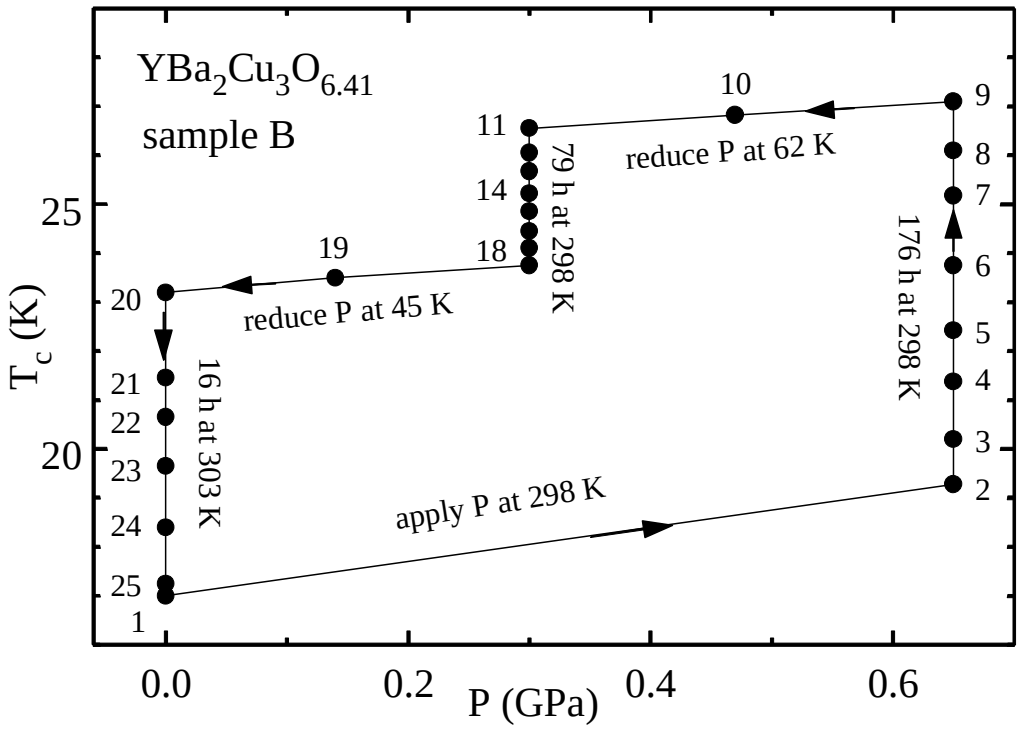
YBa2Cu3O6.41
sample B
T_c (K)
P (GPa)
25
20
0.0
0.2
0.4
0.6
1
2
3
4
5
6
7
8
9
10
11
14
18
19
20
21
22
23
24
25
reduce P at 62 K
79 h at 298 K
176 h at 298 K
reduce P at 45 K
16 h at 303 K
apply P at 298 K

Figure 3:

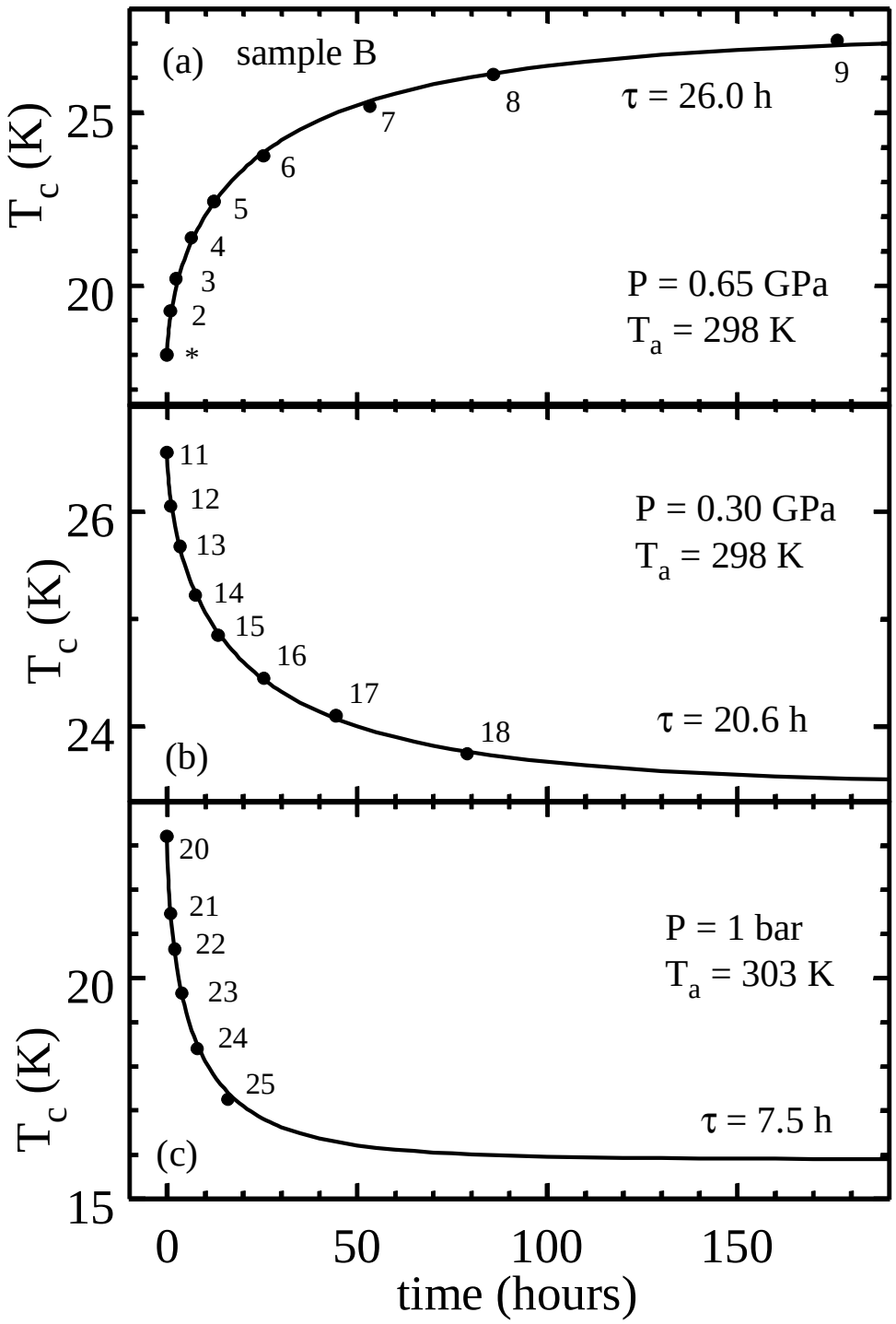
(a) sample B
τ = 26.0 h
P = 0.65 GPa
T_a = 298 K
T_c (K)
25
20
*
2
3
4
5
6
7
8
9
(b)
P = 0.30 GPa
T_a = 298 K
τ = 20.6 h
T_c (K)
26
24
11
12
13
14
15
16
17
18
(c)
P = 1 bar
T_a = 303 K
τ = 7.5 h
T_c (K)
20
15
20
21
22
23
24
25
0
50
100
150
time (hours)

Figure 4:

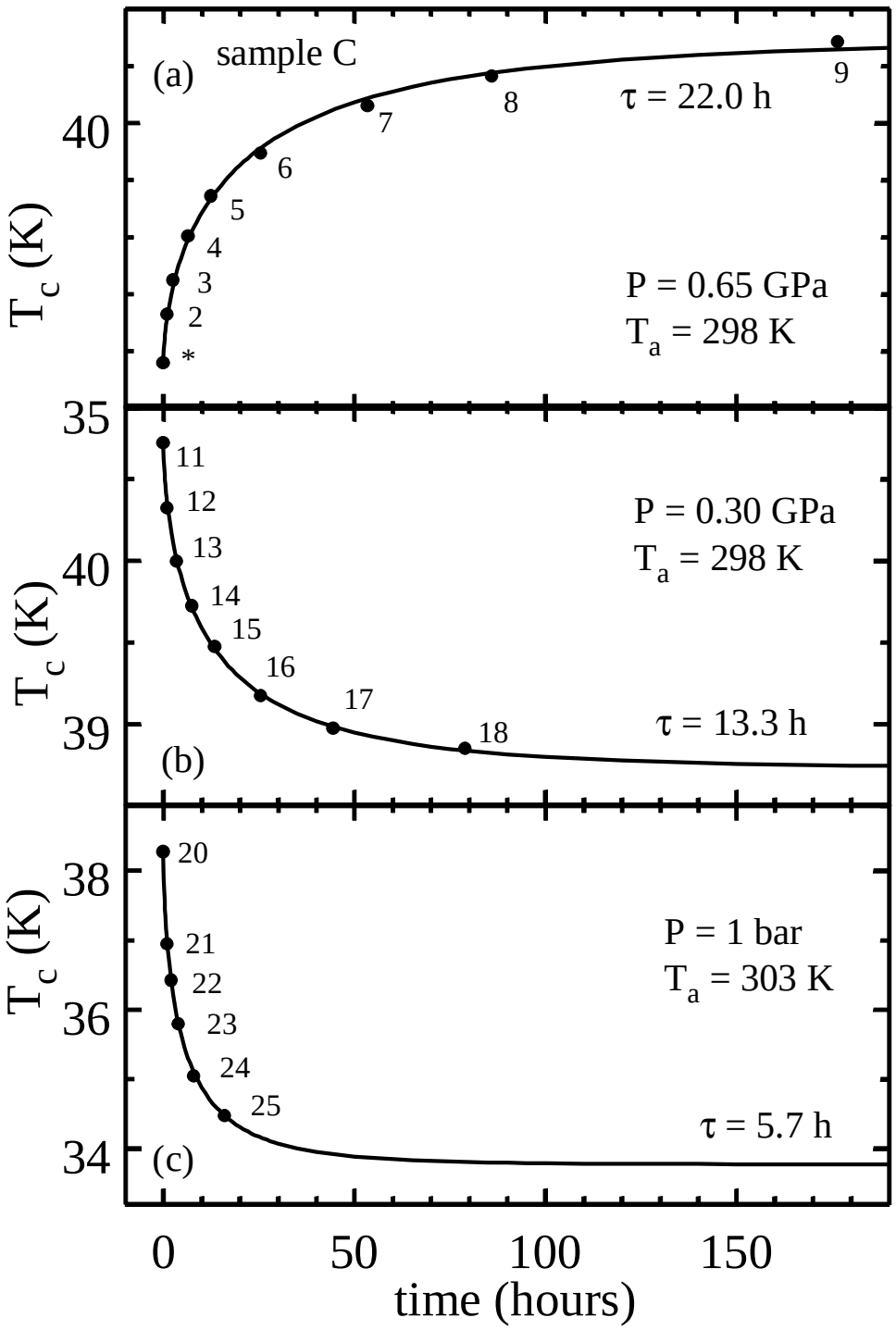
sample C
(a)
τ = 22.0 h
P = 0.65 GPa
T_a = 298 K
(b)
τ = 13.3 h
P = 0.30 GPa
T_a = 298 K
(c)
τ = 5.7 h
P = 1 bar
T_a = 303 K
T_c (K)
time (hours)
0
50
100
150
34
36
38
39
40
35
*
2
3
4
5
6
7
8
9
11
12
13
14
15
16
17
18
20
21
22
23
24
25

Figure 5:

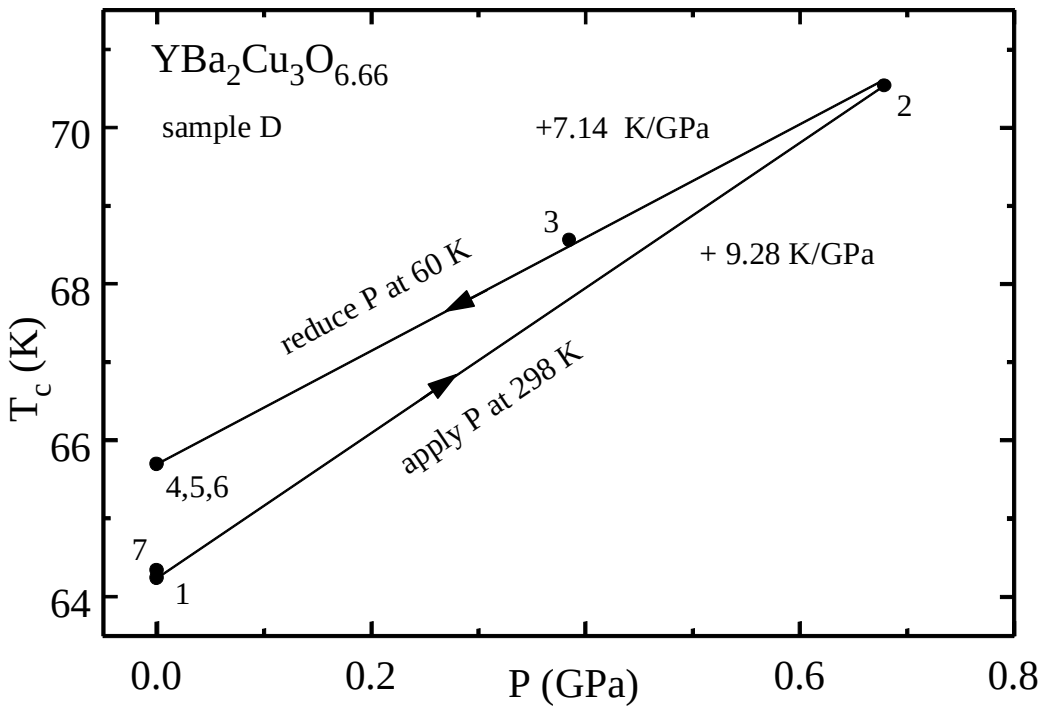
YBa2Cu3O6.66
sample D
+7.14 K/GPa
+ 9.28 K/GPa
reduce P at 60 K
apply P at 298 K
1
2
3
4,5,6
7
70
68
66
64
Tc (K)
0.0
0.2
P (GPa)
0.6
0.8

Figure 6:

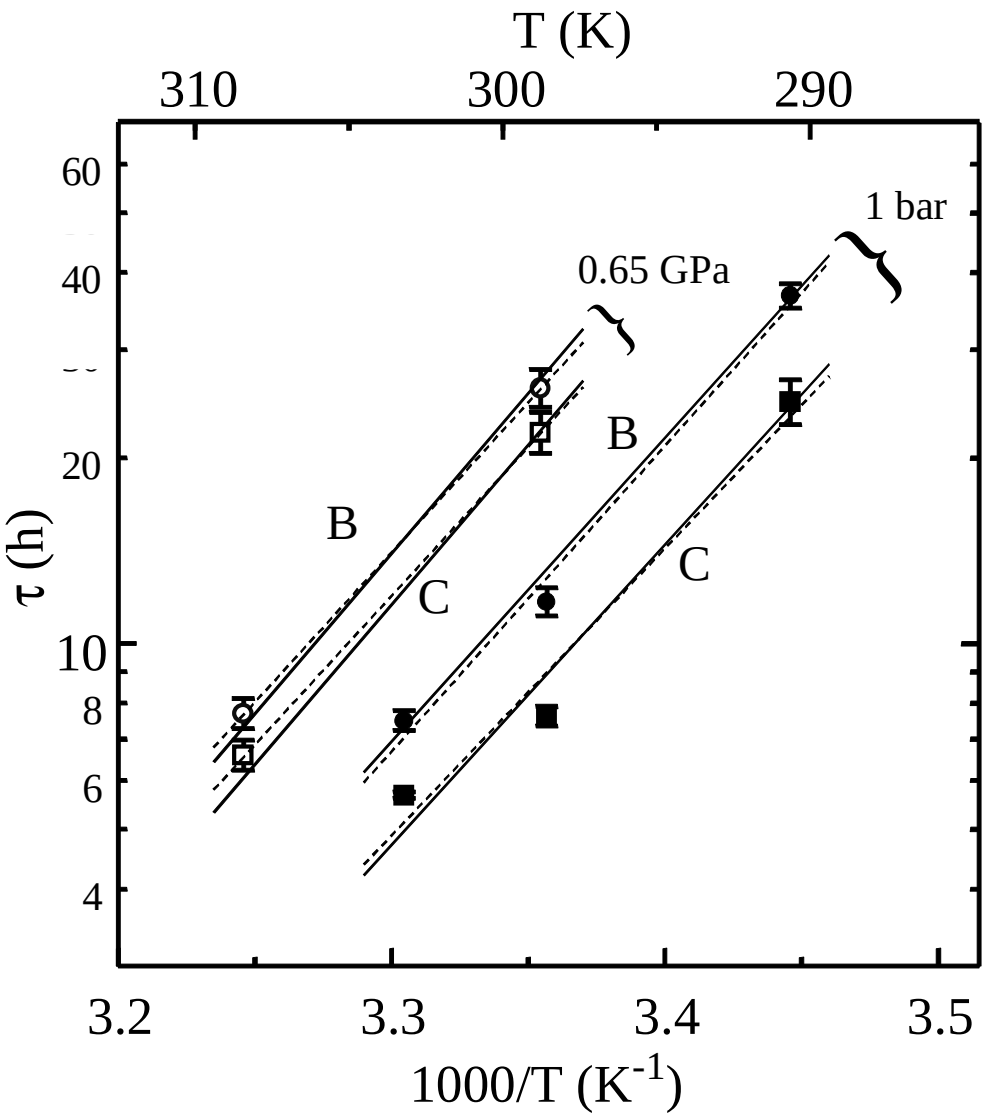
T (K)
310
300
290
60
40
20
10
8
6
4
τ (h)
1 bar
0.65 GPa
B
C
B
C
3.2
3.3
3.4
3.5
1000/T (K-1)

Figure 7:

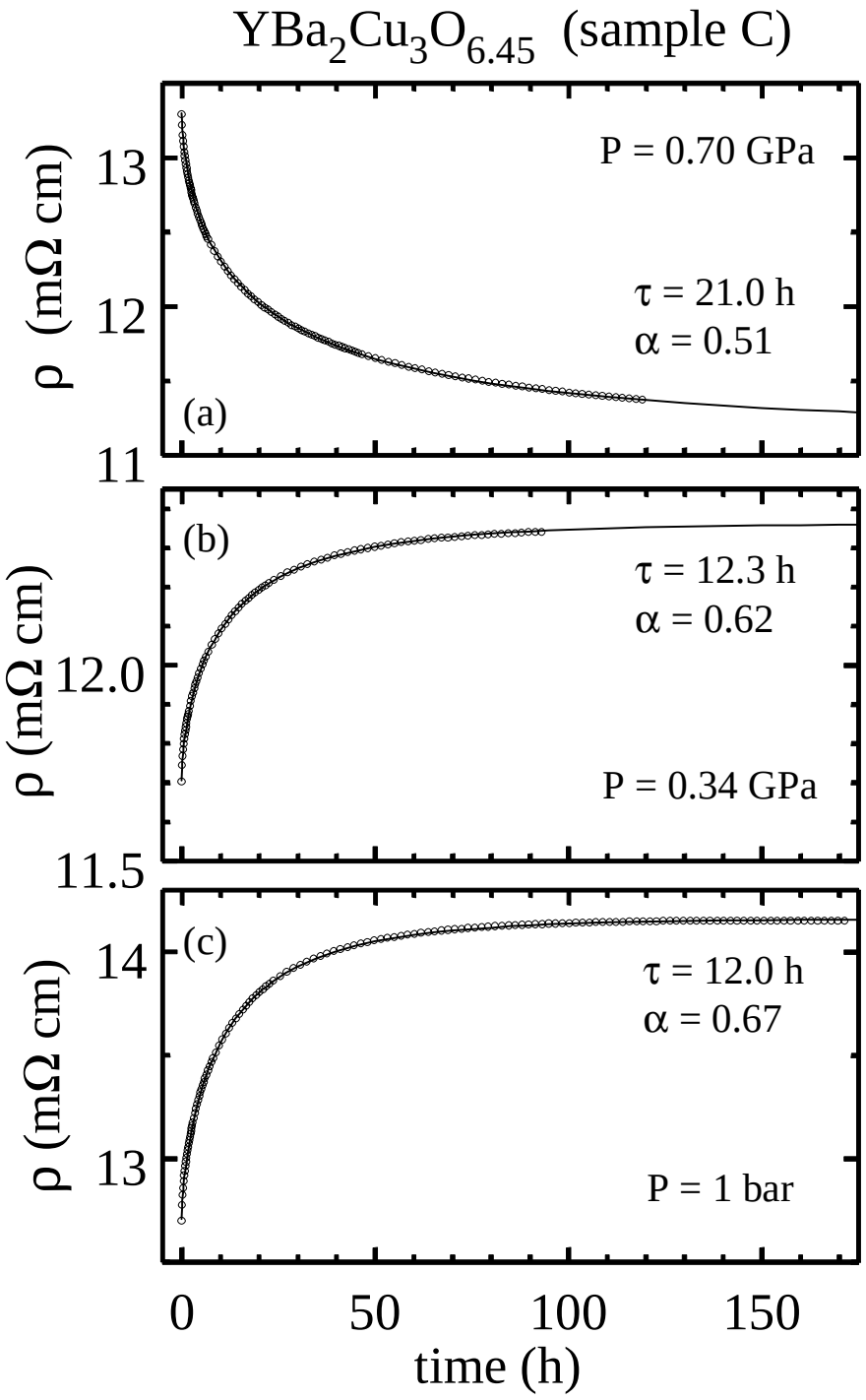
YBa2Cu3O6.45 (sample C)
P = 0.70 GPa
τ = 21.0 h
α = 0.51
(a)
ρ (mΩ cm)
13
12
11
(b)
τ = 12.3 h
α = 0.62
P = 0.34 GPa
ρ (mΩ cm)
12.0
11.5
(c)
τ = 12.0 h
α = 0.67
P = 1 bar
ρ (mΩ cm)
14
13
0
50
100
150
time (h)

Figure 8:

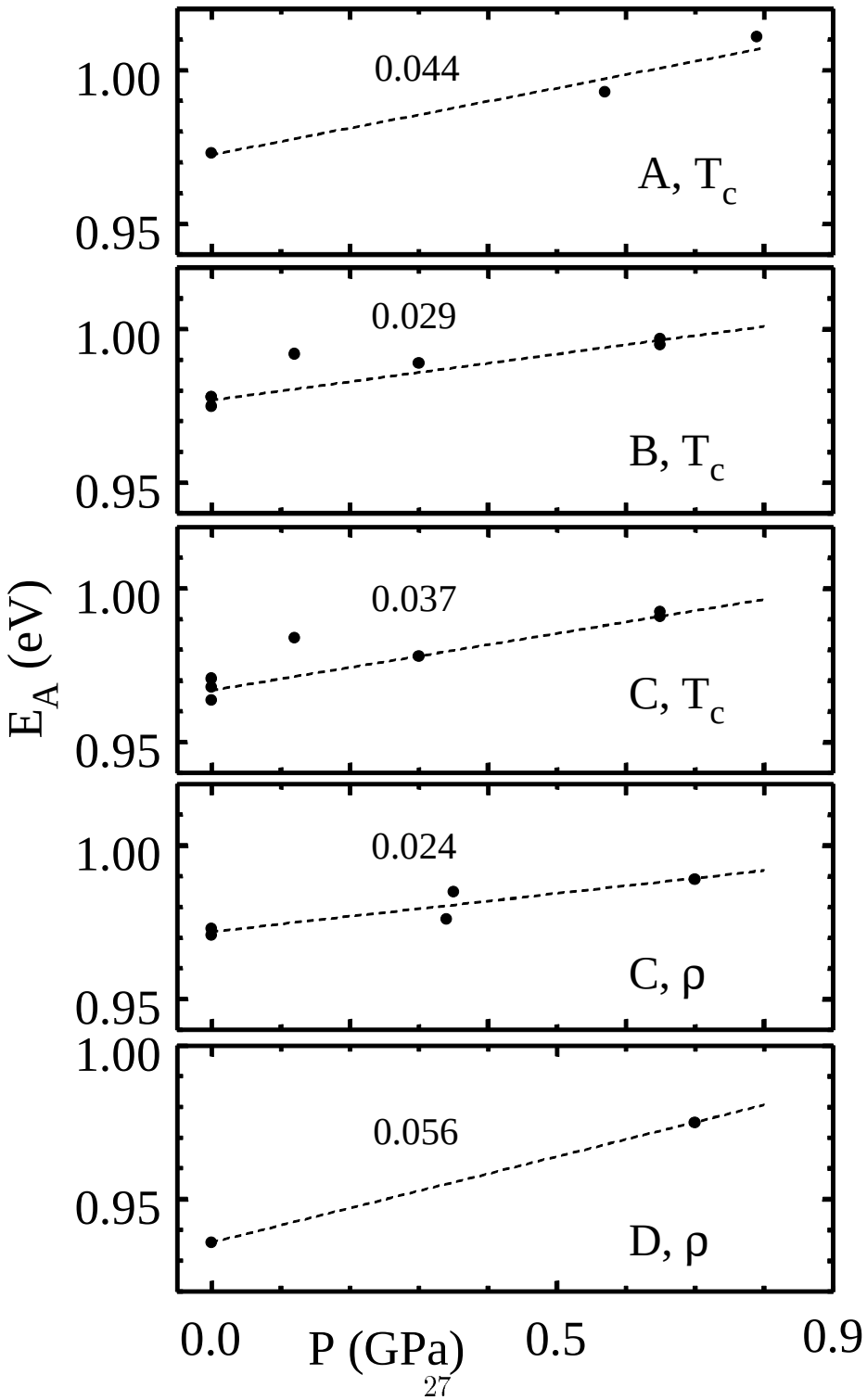
1.00
0.95
0.044
A, T$_c$
0.029
B, T$_c$
0.037
C, T$_c$
0.024
C, ρ
0.056
D, ρ
E$_A$ (eV)
0.0
P (GPa)
0.5
0.9

Figure 9: